01 Oct 2008

A New Walking Pattern SVM Technique for Five-Phase Motor Drives

Jing Huang

Keith Corzine
Missouri University of Science and Technology

Recommended Citation

J. Huang and K. Corzine, "A New Walking Pattern SVM Technique for Five-Phase Motor Drives," *Proceedings of the IEEE Industry Applications Society Annual Meeting, 2008. IAS '08*, Institute of Electrical and Electronics Engineers (IEEE), Oct 2008.
The definitive version is available at https://doi.org/10.1109/08IAS.2008.189

A New Walking Pattern SVM Technique for Five-Phase Motor Drives

Jing Huang, *Student Member, IEEE* and Keith A. Corzine, *Senior Member, IEEE*
Department of Electrical and Computer Engineering
Missouri University of Science & Technology
Rolla, MO 65409-0040

***Abstract* - As multi-phase motor drives become more popular and practical, new research in this area investigates potential advantages including lower torque ripple and better power density. The added dimensions of a multi-phase machine leads to a completely different operating nature than standard three-phase machines and merits research into new modulation methods. The five-phase and six-phase machines have been traditionally studied in the literature applying voltage-source modulation methods such as sine-triangle modulation and space-vector modulation for current harmonic elimination. Recent research of five-phase induction motor drives addressed nearest three vectors switching; which adds current harmonics but lowers torque ripple and considerably extends the drives voltage range. This paper introduces a new walking pattern SVM method which frees up the vector and sequence selection. The new method is demonstrated using detailed simulation and is shown to further reduce torque ripple.**

Keywords: five-phase; multi-phase; induction machine; space vector modulation; torque ripple; switching pattern

I. INTRODUCTION

Recently, the multi-phase motor drive system concept has become popular in some specialized applications such as electric ship propulsion, electric/hybrid vehicle traction, etc. Five-phase motor drive systems are gaining attention due to the trade-off of cost and potential advantages over the three-phase drives, such as higher power density where the weight and volume are critical and fault tolerance for better performance [1-12]. The five-phase system has some inherent characteristics which are completely different from standard three-phase systems. Most importantly, the existence of two *d-q* planes by transforming machine variables to *d-q* variables in the arbitrary reference frame splits the harmonics of system. This property can be used to design unique modulators for specific applications.

Torque ripple is the major consideration in applications where minimal acoustic noise is required. The application of a multi-phase system itself is a good way to reduce torque ripple [1-2]. Proper motor design is another popular way for torque ripple minimization [3]. Different pulse width modulation (PWM) methods have been developed in three-phase drives. However, in these systems, the torque ripple is directly related to the current wave-shape which is not the case in five-phase systems. For a five-phase system, without a zero sequence current, it is possible to have components in the currents that do not contribute to the torque. This property can be useful in lowering the torque ripple. Recent research shows that a proper vector combination can be used to reduce the torque ripple using the nearest triangle space vector modulation (SVM) [4]. Although this will increase the current THD, the current distortion may not be a disadvantage in some specific application where the torque ripple performance is the major concern. Since the SVM method requires different vector identification and sequence selection, different look-up tables are needed to determine the dwell time at different modulation indices, which increases the complexity of practical implementation. A carrier-based sine-triangle modulation method with 3rd, 5th and 7th harmonic injection has been proposed due to simple practical implementation [10].

In this paper, a new "walking pattern" SVM method is proposed. It can be easily implemented and the torque ripple and switching loss are better than the nearest triangle SVM and sine-triangle modulation with 3rd, 5th and 7th harmonic injection. A three-level five-phase inverter is used in this paper to demonstrate the proposed method. This converter integrates multilevel and multiphase technologies. Simulation of this topology is used to validate the proposed ideas.

II. FIVE-PHASE INDUCTION MACHINE AND INVERTER

Compared with the traditional three-phase induction machine, the multi-phase induction machine provides some distinct features, such as the ability to start and run even with some phases open circuited. This makes the five-phase machine attractive in systems where very high reliability is required [5]. High power density can be more easily achieved than in the case of three-phase machines by increasing the number of phases without increasing the rated current. Torque ripple behavior is also inherently superior to that of a three-phase drive system [6]. Academically, multi-phase machines can be series-connected and individually controlled from one motor drive [11-12].

To simplify the development of the five-phase induction machine model, the stator windings of all phases are assumed to be identical and coils are sinusoidally distributed. Furthermore, a linear magnetic core is considered. The inherent 72º stator winding structure causes unsymmetrical line-to-line voltages (i.e. v_{ab} and v_{ac}). For this reason the vector space does not appear in evenly distributed layers as in the case of a three-phase machine. The five-phase induction machine model used

978-1-4244-2279-1/08/$25.00 © 2008 IEEE

herein will be based on the arbitrary reference frame transformation [4]

$$\begin{bmatrix} f_{qs1} \\ f_{ds1} \\ f_{qs2} \\ f_{ds2} \\ f_{0s} \end{bmatrix} = \frac{2}{5} \begin{bmatrix} \cos(\theta) & \cos\left(\theta-\frac{2\pi}{5}\right) & \cos\left(\theta-\frac{4\pi}{5}\right) & \cos\left(\theta+\frac{4\pi}{5}\right) & \cos\left(\theta+\frac{2\pi}{5}\right) \\ \sin(\theta) & \sin\left(\theta-\frac{2\pi}{5}\right) & \sin\left(\theta-\frac{4\pi}{5}\right) & \sin\left(\theta+\frac{4\pi}{5}\right) & \sin\left(\theta+\frac{2\pi}{5}\right) \\ \cos(\theta) & \cos\left(\theta+\frac{4\pi}{5}\right) & \cos\left(\theta-\frac{2\pi}{5}\right) & \cos\left(\theta+\frac{2\pi}{5}\right) & \cos\left(\theta-\frac{4\pi}{5}\right) \\ \sin(\theta) & \sin\left(\theta+\frac{4\pi}{5}\right) & \sin\left(\theta-\frac{2\pi}{5}\right) & \sin\left(\theta+\frac{2\pi}{5}\right) & \sin\left(\theta-\frac{4\pi}{5}\right) \\ 0.5 & 0.5 & 0.5 & 0.5 & 0.5 \end{bmatrix} \begin{bmatrix} f_{as} \\ f_{bs} \\ f_{cs} \\ f_{ds} \\ f_{es} \end{bmatrix} \quad \textbf{(1)}$$

where f may represent voltage, current, or flux linkage. Transforming the machine-variable voltage and flux linkage equations to the arbitrary reference frame gives a traditional d-q model which has two d-q axes and one zero sequence that are used to represent the original five phases. The d-q model of five-phase induction machine is shown in the Figure 1. The model has been split into three parts; one part is the decoupled $d1$-$q1$ model, which has similar form as the three-phase model. The rest is $d2$-$q2$ and zero models, which have simple resistive-inductive representative equivalent circuit. It can be shown from (1) that applied voltages of harmonic $5k \pm 1$ appear in the $d1$-$q1$ plane and harmonics of $5k \pm 2$ appear in the $d2$-$q2$ plane (where k is an integer harmonic number). Furthermore, the $d2$-$q2$ plane does not contain back-EMF terms which is also noted by the torque equation

$$T_e = \frac{5}{2}\frac{P}{2}\left(\lambda_{qr1} i_{dr1} - \lambda_{dr1} i_{qr1}\right) \quad \textbf{(2)}$$

Therefore, harmonics such as the 3rd, 7th, 11th, 13th, etc. do not contribute to electromagnetic torque.

The five-phase induction motor is generally driven by a two-level voltage-source inverter [4, 5]. Figure 2 shows the diagram of the system. The two d-q vector plots of five-phase two-level are also shown in the Figure 2. There is one vector in each of the vector planes corresponding to the same switching state, and they are plotted in the same color. It can be seen that the vectors are located on three circles in each plane, in addition to the zero vectors at the origin. It is interesting to note that vectors on the inner circle of the $d1$-$q1$ plane correspond to those on the outer circle of the $d2$-$q2$ plane, and vice versa. This feature could be utilized to achieve an optimal modulation to reduce torque ripple and current harmonics [4].

Acoustic noise caused by torque pulsation has been a major concern in certain applications. One technique to alleviate the situation is to use multilevel motor drive systems, which have more discrete switching states to achieve a smoother voltage waveform. A typical five-phase three-level diode-clamped inverter drive system is shown in Figure 3, which is a natural extension of the common three-phase counterpart. With more voltage levels, the number of switching states increases dramatically, as can be seen in the voltage vector plots in the $d1$-$q1$ and $d2$-$q2$ vector planes. Some corresponding vectors in both planes are also plotted in the same color to show their relationship. It can be seen that although the relationship between corresponding vectors is more complicated than in the two-level system, the same rule still holds that, in general, outer vectors in one plane correspond to inner vectors in the other.

With a star-connected motor, it can be shown that the motor voltages are related to the inverter line-to-ground voltage by

$$\begin{bmatrix} v_{as} \\ v_{bs} \\ v_{cs} \\ v_{ds} \\ v_{es} \end{bmatrix} = \frac{1}{5} \begin{bmatrix} 4 & -1 & -1 & -1 & -1 \\ -1 & 4 & -1 & -1 & -1 \\ -1 & -1 & 4 & -1 & -1 \\ -1 & -1 & -1 & 4 & -1 \\ -1 & -1 & -1 & -1 & 4 \end{bmatrix} \begin{bmatrix} v_{ag} \\ v_{bg} \\ v_{cg} \\ v_{dg} \\ v_{eg} \end{bmatrix} \quad (3)$$

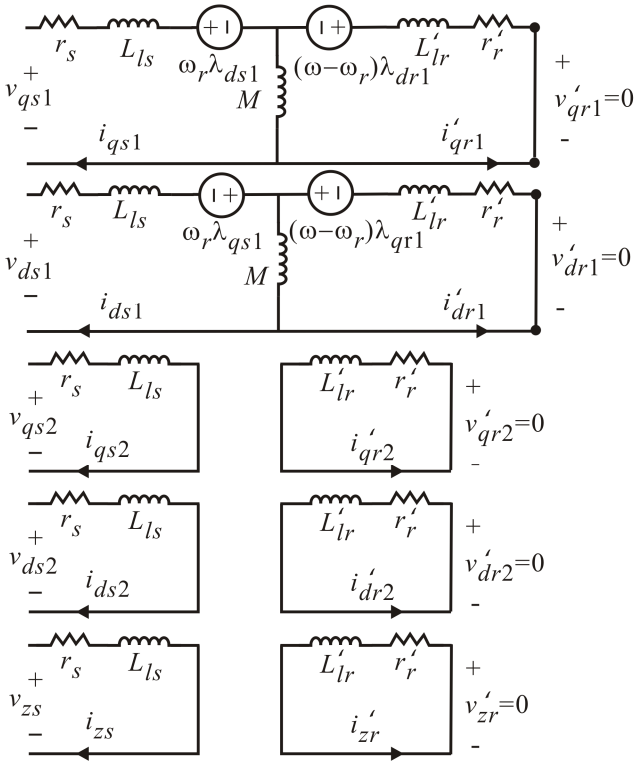

Figure 1. The dq models of five-phase induction motor and vector plots.

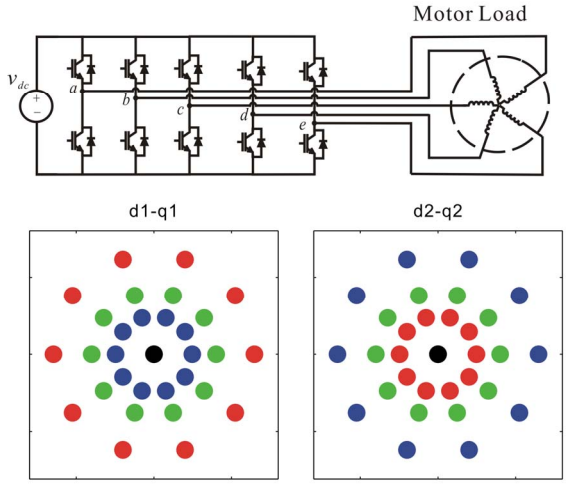

Figure 2. Two-level five-phase motor drive system and vector plot.

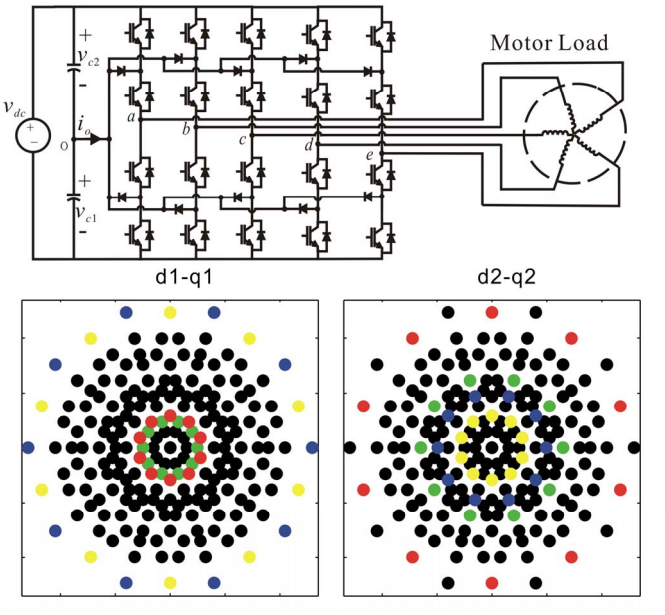

Figure 3. Three-level five-phase motor drive system and vector plot.

III. Walking Pattern SVM Theory

Considering the large number of available voltage vectors, the number of possible SVM patterns is unlimited. In traditional multilevel drive systems, the three voltage vectors nearest the commanded voltage are selected, modulation times are calculated, and a switching sequence is followed [13-15]. Herein, a new "walking pattern" concept is introduced. Using this technique, there is no restriction to the nearest vectors. Instead, vector selection is chosen so that the pattern "walks" around the commanded voltage. The angle about which the switching moves around the commanded voltage is first determined with the goal of minimizing the torque ripple. This is accomplished by using the induction machine model shown in Figure 1 with a disturbance added to the $q1$- and $d1$-axis voltages at the rated operating point. The $q1$-$d1$ voltage disturbances can be expressed as shown in Figure 4a using

$$\Delta v^{e}_{qs1} = k v_s \cos(\phi_v)\sin(\omega_s t)$$
$$\Delta v^{e}_{ds1} = -k v_s \sin(\phi_v)\sin(\omega_s t) \quad \textbf{(4)}$$

where k is a small factor representing a percentage of the RMS phase voltage v_s and ω_s is and injection frequency which can be set to the expected modulation carrier frequency. By varying the injection angle ϕ_v (shown in Figure 4b), a corresponding torque ripple can be calculated.

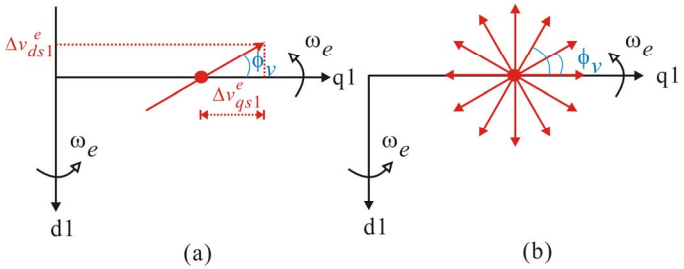

Figure 4. Disturbance signal in $q1$-$d1$ vector space.

Figure 5 shows the resulting torque ripple as the injection angle is varied from 0 to 360°. It is seen that the torque ripple reaches a minimum when the switching angle is 72° or 252°. It should be pointed out that the fundamental component of the voltage is placed in the $q1$-axis and, therefore, the optimal injection angle is defined as 72° or 252° from the radial direction of the commanded voltage. These optimal angles are used as a guideline for the voltage-source modulation. As an example, Figure 6 shows the vector plot with a walking pattern. The circle represents the ideal commanded voltage when the modulation index is set to 1.1212. Points along the commanded voltage are selected which are in-between available vectors. The vectors are chosen so that the angle formed by switching between them creates switching ripple at approximately 72° or 252°. For example, the commanded voltage "*A*" could be obtained by switching to vector 191 and 218 with some pre-calculated dwell time. Also, by selecting vectors with sequence 191→218→191→218, the torque ripple decreases with sacrificing of switching loss. Therefore, there is a tradeoff between the torque ripple and switching loss when deciding the back and forth times along the 72 and 252 degree direction line (vector moving direction line).

It should be noted that the optimal angle that gives the minimal torque ripple should be between the walking pattern line and the commanded voltage vector, not the $q1$-axis. In Figure 6, the angle is shown to be between two lines, one connecting vectors 191 and 218, and the other connecting the origin and vector A.

Although the study shown in Figure 4 indicates that the optimal angle is 72 or 252 degrees, it has been proven through simulation that the angle may be different for other operating points. In addition, it may not possible to find state vectors near the commanded voltage vector that can give the exact angle. However, from Figure 6 it can be seen that if the optimal angle can not used, other angles close to it also yield low torque ripple. Therefore, in practice one should choose the switching state that forms an angle most close to the optimal one.

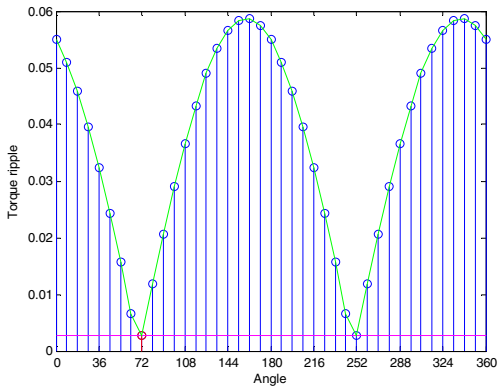

Figure 5. Relationship between torque ripple and angle.

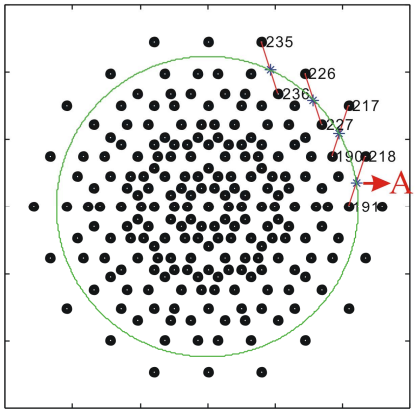

Figure 6. Fundamental concept of walking pattern SVM.

The vectors are selected and the switching times are calculated for one-fifth of a fundamental cycle. For the remainder of the cycle, the pattern can be repeated with phases transposed. Note that the average voltages made up by this pattern are not evenly spaced along the commanded voltage path, but instead depend on the specific vectors selected. Calculation of the vector times ensures that the modulated voltage equals the commanded voltage on average.

To implement the proposed technique, the optimal switching patterns can be pre-calculated and stored in a look-up table for fast retrieval. Although there are many switching states for the multilevel multi-phase system, the actual table size can be greatly reduced by taking vector symmetry into account.

If the controller's data storage memory is very limited, the patterns can also be determined online in each control cycle with calculation. This implementation was adopted in this study. First the crossing point will be numerically solved from the expression of the commanded voltage circle and each path line segment. Then the dwelling time of each vector will be decided by the distance between the commanded voltage and each vector along the path line segment, since only two vectors are used to from the commanded voltage.

IV. Various SVM Walking Patterns

In this paper, several "walking patterns" are examined to determine the modulation methods with minimal torque ripple. Figures 7a through 7d show some examples of different walking patterns. As can be seen, the intersection of the "walking loop" and the reference voltage will cause different switching numbers. The general closest triangle SVM is plotted in Figure 7e. The sine-triangle PWM modulation with 3rd, 5th and 7th harmonics injection is also plotted in Figure 7f as a comparison [10]. Table 1 shows the comparison results.

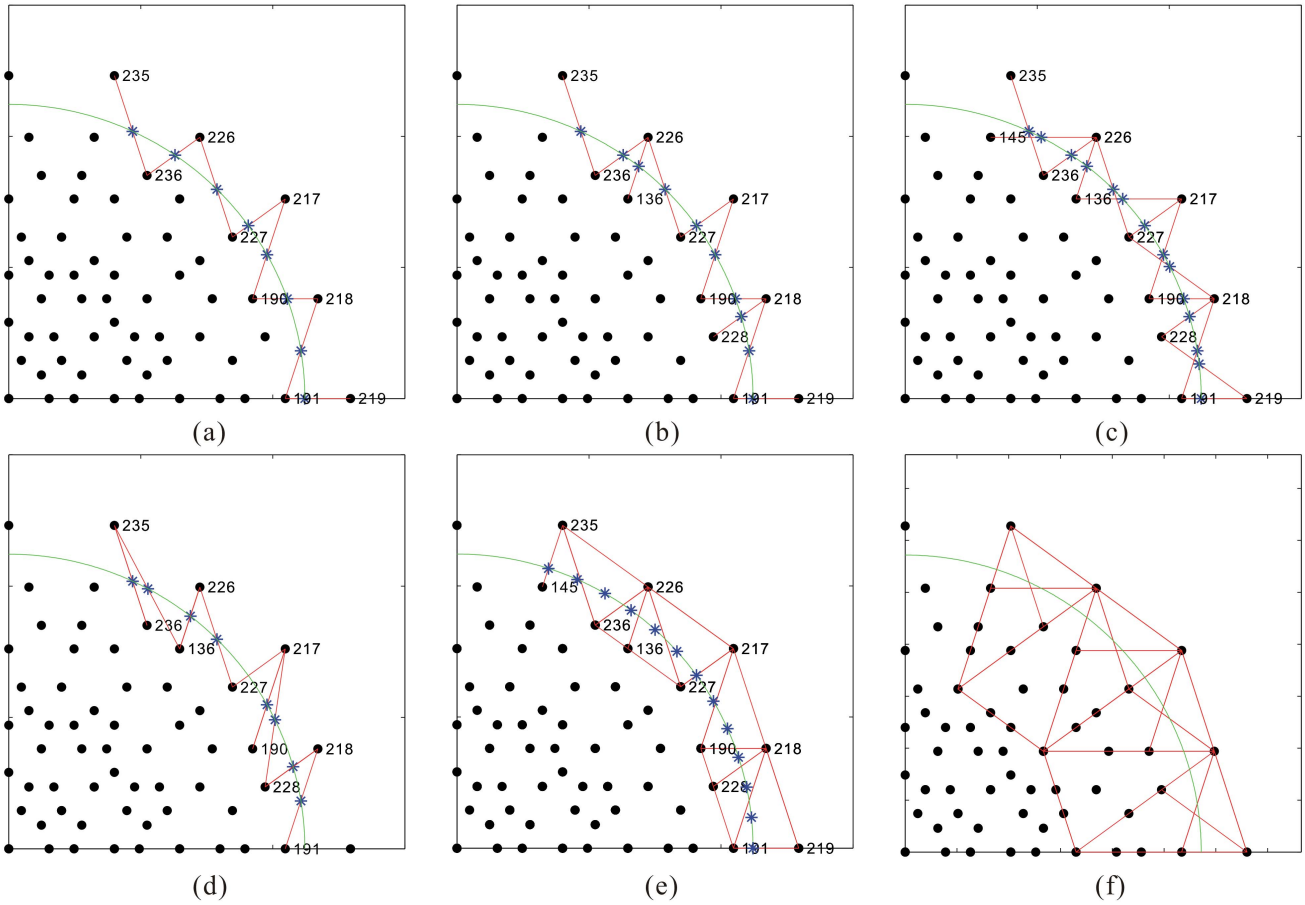

Figure 7. Various switching state selection.

Table 1. Torque ripple and switching frequency of various switching state selection.

	Torque ripple (in percent)	Corresponding Switching frequency
Walking pattern-1 (a)	1.35%	2680 Hz
Walking pattern-2 (b)	1.02%	3640 Hz
Walking pattern-3 (c)	1.37%	5080 Hz
Walking pattern-4 (d)	1.62%	3400 Hz
Nearest triangle SVM (e)	1.66%	3644 Hz
Sine-triangle PWM (f)	2.78% More cases are shown in Figure 8.	3600 Hz More cases are shown in Figure 8.

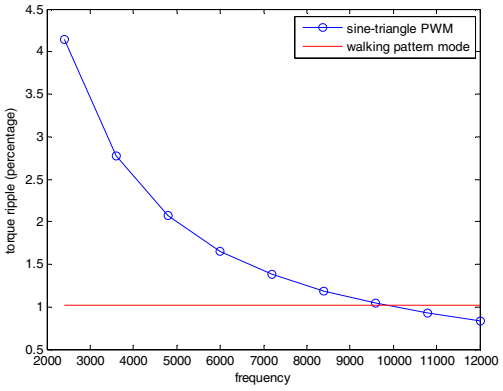

Figure 8. Relationship between torque ripple and switching frequency.

Table 1 shows that walking pattern-2 SVM has the minimum torque ripple among all the walking patterns. For sine-triangle PWM, the commanded voltage is distributed along the reference circle evenly, so the torque ripple and switching number are dependant on the switching frequency. Figure 8 shows the with same level torque ripple, a switching frequency of 9.9-kHz will be required. The walking pattern-2 has only 61 switching number per phase per period, which translates to a transistor switching frequency of 3.66 kHz. Compared to the closest triangle SVM, the torque ripple of

walking pattern-2 reduces by 38% while the switching losses are the same.

V. Analysis of Walking Pattern SVM

To further analyze the effects of different walking patterns on the system's torque ripple performance, a detailed analysis was carried out on walking pattern-2 within a time window of 1/5 of a fundamental cycle. The vector sequence was chosen to be:

219→191→219→191→218→191→218→191→218→228→
218→228→218→190→218→190→217→190→217→190.

Figure 9 shows the switching states for each phase. It can be seen that as the selected vector change from one to another, the switching state of each phase can be 0, 1 or 2. Also Figure 9 includes the torque waveform to show the effects of switching patterns. The dwell times of each switching vector were also calculated and listed in Table 2.

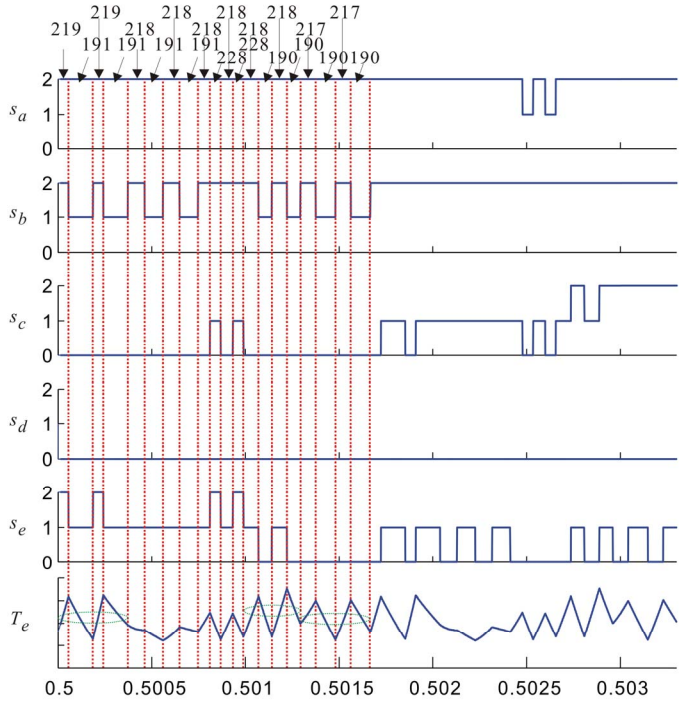

Figure 9. Switching state for walking pattern-2 SVM

As can be seen, the effects of different switching patterns on the torque change are quite obvious. For example, the two vectors 219 and 191 form a zero degree angle with respect to the commanded voltage vector, and large torque variations can be observed when the switching state changes from one vector to the other. On the other hand, vectors 191 and 218 form an angle with respect to the commanded vector that is close to 72 degree, and the corresponding torque variations are quite small. Similar small torque changes can be observed for vectors 218 and 228, which also form an angle that is close to 72 degrees. Again, vectors 190 and 218 has an angle far from 72 degrees, torque ripple is big during these vector switching.

It should be pointed out that switching vector angle is not the only factor that affects output torque ripple. The other major contributor is the distance between the switching vectors and the commanded voltage vector. Switching vectors that are closer to the commanded vector usually produce smaller torque ripple. This can be illustrated by looking at vectors 228-217 in Figure 7d and vectors 190-218 in Figure 7b. Although the former pair forms an angle that is closer to 72 degrees, their long distance from the commanded vector make the output torque variation is even higher than that caused by the latter vector pair. Therefore, minimizing output torque ripple requires choosing switching vectors that are close the commanded vector and have an angle that is close to the optimal angle.

An extensive set of simulations was done to determine the optimal angles that give the minimal torque ripple at various operating points. Figure 10 shows that for different motor speed (slip), torque, and modulation index, the optimal angle differs. However, it can also be seen that the angles only change in a small range. Given the limited options in choosing switching vectors, they are likely to correspond to the same walking pattern path. Although in some conditions, a new walking pattern path is needed for minimum torque ripple.

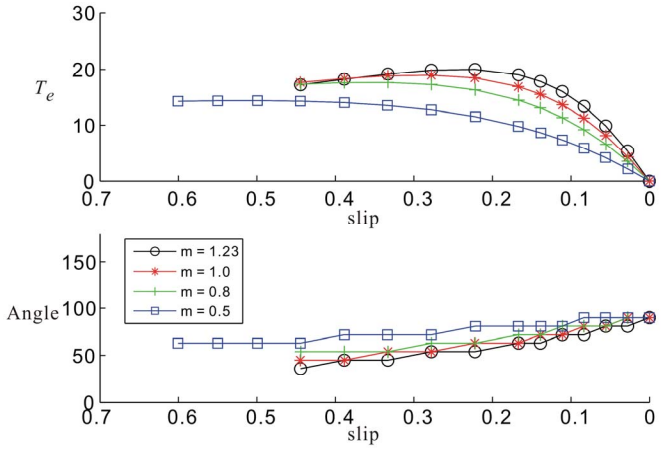

Figure 10. Switching state for walking pattern-2 SVM

Table 2. Dwell time of each vector for walking pattern-2.

Vector	219	191	219	191	218
dt (ms)	0.0557	0.1304	0.0557	0.1304	0.0895
Vector	191	218	191	218	228
dt (ms)	0.0976	0.0895	0.0976	0.0644	0.0571
Vector	218	228	218	190	218
dt (ms)	0.0644	0.0571	0.0804	0.0713	0.0804
Vector	190	217	190	217	190
dt (ms)	0.0713	0.0825	0.1046	0.0825	0.1046

Although it is difficult to determine analytically the optimal angle under various operating conditions, it is possible to establish a relationship through vast amount of simulation data.

One potential method of readily obtaining the optimal angle is to train neural networks to learn the mapping relationship based on a small set of simulation data.

VI. Simulation Verification

For a more detailed observation, the simulated voltage, current, and torque of walking pattern -2 and the nearest triangle SVM are plotted in Figure 11. The sine-triangle PWM modulation with 3rd, 5th and 7th harmonics injection [10] and sine-triangle PWM modulation without harmonics injection are also simulated as comparison.

The fundamental phase voltage is 57.07V in case d, the fundamental current is 2.08A, and the average torque is 1.12N·m. The operation in the other cases make these fundamental and average values the same as in the d case. However, decreasing torque ripple can be observed from Figure 11a to Figure 11d. Compared with the sine-triangle modulation without harmonics injection method, the sine-triangle PWM with harmonic injection method can achieve a torque ripple level that is 62.3% lower, the corresponding value is 37.3% for the nearest triangle SVM method and 22.9% for the walking pattern-2 SVM method.

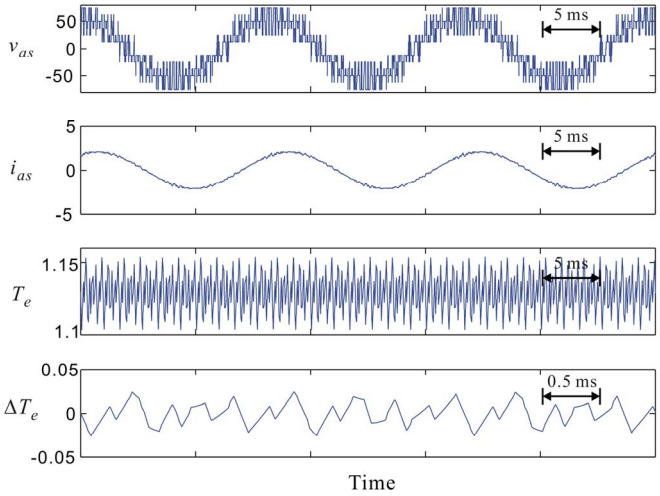

(a) Sine-triangle modulation without harmonics injection.

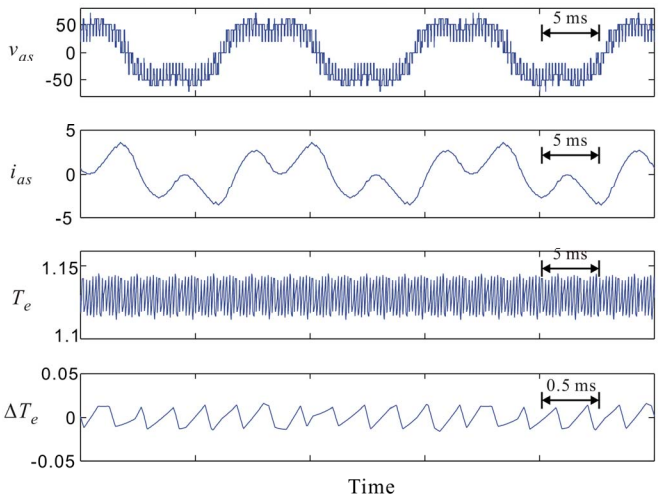

(b) Sine-triangle modulation with harmonic injection.

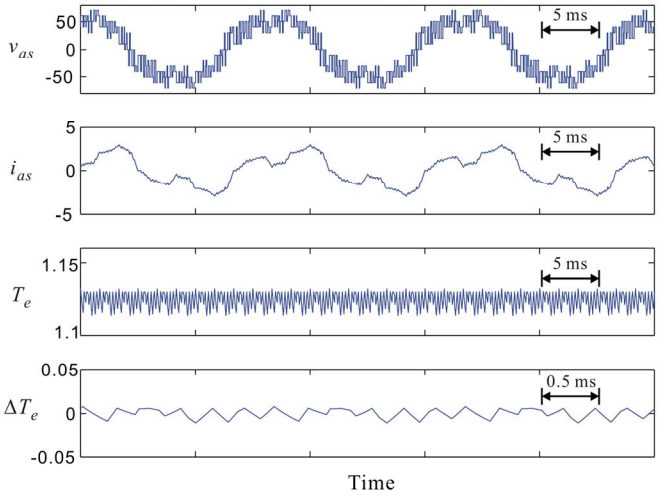

(c) Nearest triangle SVM.

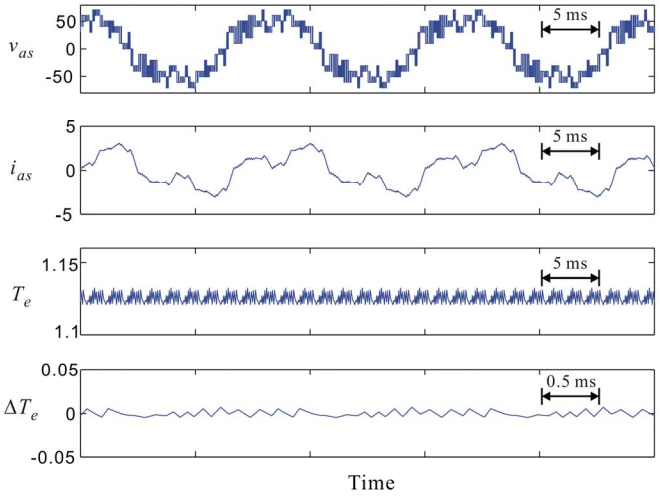

(d) Walking pattern-2 SVM.

Figure 11. Simulation comparison of different modulation method.

VII. Conclusion

This paper presents a new SVM method for five-phase induction motor drives. Unlike other SVM methods, the vectors are not constrained to nearest vectors; but instead follow a "walking pattern" about the reference voltage. Simulation results show that the new SVM pattern results in reduced torque ripple and reduced switching frequency when compared with other methods.

References

[1] L. Parsa and H.A. Toliyat, "Five-Phase Permanent Magnet Motor Drives," *IEEE Transactions on Industry Applications*, volume 41, pages 30-37, January/February 2005.

[2] H.A. Toliyat, L. Xu and T.A. Lipo, "A Five Phase Reluctance Machine with High Specific Torque," *IEEE Transactions on Industry Applications,* volume 28, pages 659-667, May/June 1992.

[3] L. Parsa, H.A. Toliyat, and A. Goodarzi, "Five-Phase Interior Permanent-Magnet Motors With Low Torque Pulsation," *IEEE Transactions on Industry Applications*, volume 43, number 1, pages 40-46, January/February 2007.

[4] S. Lu and K.A. Corzine, "Multilevel Multi-Phase Propulsion Drives," *IEEE Electric Ship Technologies Symposium,* July 2005.

[5] H. Xu, H.A. Toliyat, and L.J. Peterson, "Five-phase induction motor drives with DSP-based control system," *IEEE Transactions. on Power Electronics,* volume 17, number 4, pages 524-533, 2002.

[6] R. Shi and H.A. Toliyat, "Vector control of five-phase synchronous reluctance motor with space vector pulse width modulation (SVPWM) for minimum switching losses," *IEEE Applied Power Electronics Conference*, pages 57-63, 2002.

[7] A. Iqbal and E. Levi, "Space vector modulation scheme for a five-phase voltage source inverter," *Proceedings of the European Power Electronics Conference,* Dresden, Germany, 2005.

[8] A. Iqbal, E. Levi, M. Jones, and S.N. Ukosavic, "A PWM Scheme for a Five-Phase VSI Supplying a Five-Phase Two-Motor Drive**,"** *Proceedings of the IEEE Industrial Electronics Conference,* pages 2575-2580, November 2006.

[9] O. Ojo and D. Gan, "Generalized discontinuous carrier-based PWM modulation scheme for multi-phase converter-machine systems," *Proceedings of the IEEE Industry Applications Society Conference,* volume 2, pages 1374-1381, 2005.

[10] J. Huang, K.A. Corzine, C.M. Hutson, and S. Lu, "Extending Voltage Range and Reducing Torque Ripple of Five-Phase Motor Drives with Added Voltage Harmonics," *Proceedings of the IEEE Applied Power Electronics Conference,* February 2008.

[11] E. Semail, E. Levi, A. Bouscayrol, X. Kestelyn, "Multi-machine modelling of two series connected 5-phase synchronous machines: effect of harmonics on control Semail," *IEEE Power Electronics and Applications Conference*, September 2005.

[12] E. Levi, M. Jones, S.N. Vukosavic, and H.A. Toliyat, "Steady State Modeling of Series-Connected Five-Phase and Six-Phase Two-Motor Drives, " *IEEE Industry Applications Conference,* volume 1, pages 415-422, October 2006.

[13] N. Celanovic and D. Boroyevich, "A fast space-vector modulation algorithm for multilevel three-phase converters," *IEEE Transactions on Industry Applications*, volume 37, pages 637-641, March/April 2001.

[14] M. Koyama, T. Fujii, R. Uchida, T. Kawabata, "Space voltage vector-based new PWM method for large capacity three-level GTO inverter," *IEEE Industrial Electronics Conference*, pages 271-276, November 1992.

[15] S.B. Seok, G. Sinha, M.D. Manjrekar, and T.A. Lipo, "Multilevel Power Conversion - An Overview Of Topologies And Modulation Strategies," *Proceedings of the 6th International Optimization of Electrical and Electronic Equipments Conference*, volume 2, pages AD-11 - AD-24, May 1998.